Optical and Photocatalytic Properties of Copper(II) Doped Zinc Oxide

MARIUS RADULESCU[1], LAURA VASILICA ARSENIE[1], OVIDIU OPREA[1]*, BOGDAN STEFAN VASILE[1]
[1]University Politehnica of Bucharest, Faculty of Applied Chemistry and Materials Sciences, 1 Gh. Polizu, Bucharest, Romania

The aim of the present study was the synthesis and characterization of copper(II) doped zinc oxide. The synthesis was done by solvothermal method, in 1-butanol or 1-pentanol, using only the acetate of the corresponding metal. The characterization of the obtained powders was done by X-ray diffraction (XRD), transmission electron microscopy (TEM), thermal analysis (TG-DSC), UV-Vis and fluorescence spectra (PL). The determination of the optical properties have indicated that while the UV-Vis absorbtion remains high, the photocatalytic activity is strongly diminished by the presence of the copper ions. Such nanoparticles are therefore best candidates for textile industry or cosmetic industry, where the usual photocatalytic activity of ZnO is a major drawback.

Keywords: ZnO, photocatalytic activity, optical, copper

ZnO, together with other metal oxides like Fe_3O_4 or TiO_2, is one of the workhorses of today chemistry [1-3]. The main reason for this high interest is the great number of application domains for these nanoparticles. We can mention here some of its uses in: paints [4-7], electronics [7-13], catalysis [14-16], rubber industry [17-19], cosmetics [20-25], textile industry [23, 26-28]. At the base of ZnO nanoparticles versatility are few well-known properties: a 3.23eV band-gap, which is at the limit of UV and visible domains, high UV absorbtion capacity coupled with low visible light absorbtion, very good stability in time, non-toxic character and high photocatalytic activity [29-31].

Some of the well-known applications of ZnO nanoparticles are in textiles industry or in cosmetics as a UV blocking filter to protect the fabric or the skin from the harmful radiation. One problem that limits this application is the photocatalytic activity of ZnO, which is high enough to degrade overtime the same fabric or the skin cells that was meant to protect [32, 33]. These are the reasons why we focused on obtaining ZnO nanoparticles with good UV absorbance, but with low photocatalytic activity.

In this paper we report for the first time to our knowledge the obtaining of ZnO nanoparticles, with negligible photocatalytic activity, but with high UV absorbance, properties that makes them suitable as UV shield in various applications.

Experimental part

Zinc acetate dihydrate, $Zn(CH_3COO)_2 \cdot 2H_2O$ and $Cu(CH_3COO)_2 \cdot H_2O$ with 99% purity was obtained from Sigma Aldrich. Absolute ethanol was used as received from Sigma without further purification.

ZnO synthesis: 2.1940g (0.01 moles) $Zn(CH_3COO)_2 2H_2O$ were dissolved in 50 mL 1 butanol or 1-pentanol. The solution was then kept for 24h on a thermostatic bath at 80°C. The white colloidal precipitate that formed was separated by centrifugation at 12.000 rpm and washed several times with ethanol. Final product was dried at 105°C for 30 min then calcined at 300°C for 2h.

The 1, 3, 5 and 10% copper doped ZnO samples were prepared in a similar manner, by adding the corresponding $Cu(CH_3COO)_2 \cdot H_2O$ quantity over the $Zn(CH_3COO)_2 \cdot 2H_2O$ in the beginning of the synthesis.

Methods

a) Electron Microscope Images. The transmission electron images were obtained on dried, finely powdered samples using a Tecnai™ G² F30 S-TWIN high resolution transmission electron microscope from FEI, operated at an acceleration voltage of 300 KV obtained from a Shottky Field emitter with a TEM point resolution of 2 Å and line resolution of 1.02 Å.

b) X-ray Diffraction. X-ray powder diffraction patterns were obtained with a Shimadzu XRD6000 diffractometer, using Cu Kα (1.5406 Å) radiation operating with 30 mA and 40 kV in the 2θ range 10–70°. A scan rate of 1° min^{-1} was employed.

c) Thermal analysis. Thermal behavior of the precursors was followed by TG-DSC with a Netzsch TG 449C STA Jupiter. Sample was placed in alumina crucible and heated with 10K· min^{-1} from room temperature to 900° C, under the flow of 20 mL min^{-1} dried air.

d) Photoluminescence spectra. Photoluminescence spectra (PL) were recorded with a Perkin Elmer P55 spectrometer using a Xe lamp as a UV light source at ambient temperature, in the range 350-600 nm, with all the samples in solid phase. The measurements were made with scan speed of 200 nm·min^{-1}, slit of 10 nm, and cut-off filter of 1%. An excitation wavelength of 325 nm was used.

e) Diffuse reflectance spectra measurements were made with a JASCO V560 spectrophotometer with solid sample accessory, in the domain 200-800 nm, with a speed of 200 nm·min^{-1}.

f) The photocatalytic activity of nanopowders was investigated towards a methyl orange (MO) solution (20 mg/L) as model contaminant. Samples of pure and doped ZnO (10 mg) were suspended in 10 mL methyl orange solution and kept for 30 min under dark to reach the adsorption equilibrium. The samples were afterwards irradiated with a UV lamp (25W; 365nm). The change in MO concentration was investigated by monitoring the maximum absorbance at 464 nm, at predetermined time intervals, with an UV-Vis spectrometer. A control sample (only MO solution) was used to monitor the direct photodecomposition of the dye.

* email: ovidiu73@yahoo.com

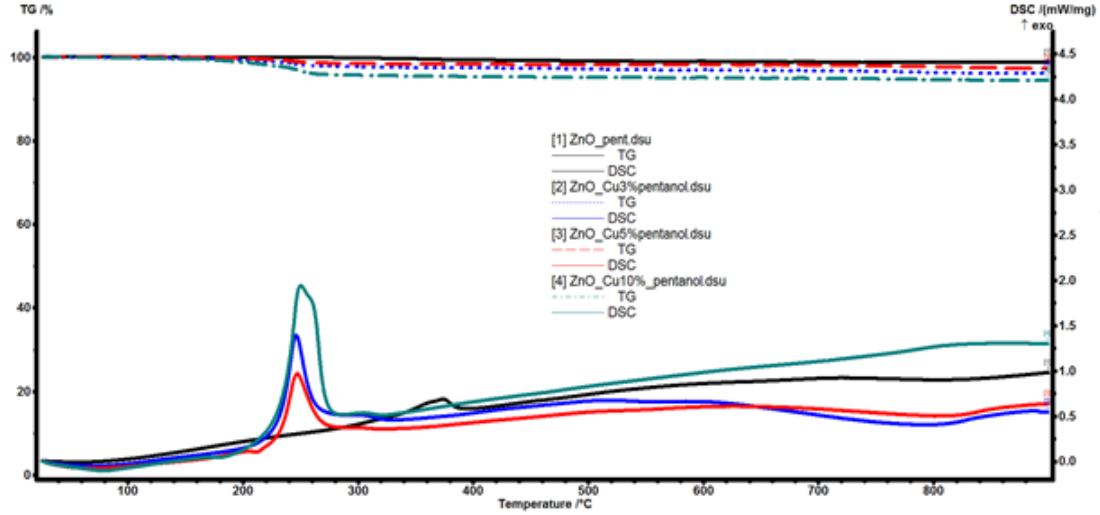

Fig. 1. TG-DSC curves for the obtained pure and doped ZnO nanoparticles in 1-pentanol

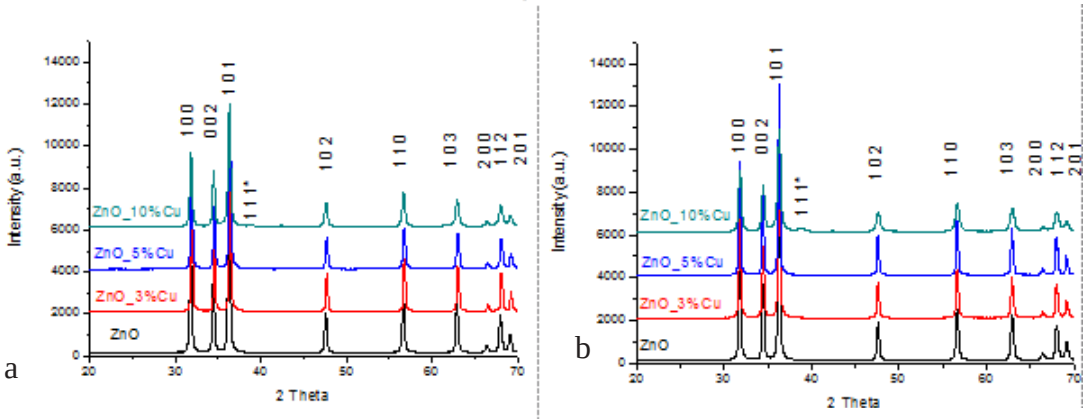

Fig. 2. XRD patterns of undoped ZnO and Cu-doped ZnO powder samples at different doping levels 1, 3, 5 and 10%, synthetized from 1-butanol (A) and in 1-pentanol (B)

Results and discussions

The thermal analysis (fig. 1) was used to monitor the formation of ZnO nanoparticles. As it can be observed the mass loss of the obtained powders is slightly increasing as the percentage of copper acetate added in synthesis is higher, indicating the fact that some of the acetate ions are still present. The calcination temperature of 300°C was chosen based on the thermal analysis.

The crystalline phase formation was investigated by X-ray diffraction. The XRD data presented in figure 2A and 2B demonstrate the formation of ZnO as final product [ASTM 079-0205].

All patterns can be indexed to a hexagonal wurtzite structure. The XRD patterns show that there was a second-phase peak only for 10%Cu samples, where (111) of CuO can be identified. Nevertheless, we can state that the doping process did not change the wurtzite structure of ZnO.

The crystallite size of the samples can be estimated from the Scherrer equation, $D = 0.89 \cdot \lambda / \beta \cdot \cos\alpha\theta$, where D is the average grain size, λ is the X-ray wavelength (0.15405 nm), θ and β are the diffraction angle and FWHM of an observed peak, respectively. The strongest peak (101) was used to calculate the average crystallite size (D) of ZnO particles (table 1).

The average crystallite size is in general smaller for the samples obtained in 1-pentanol than for the samples synthetized in 1-butanol. For both syntheses the 10%Cu sample has the smallest crystallite size, most probably due to the saturation of the ZnO lattice with Cu^{2+} ions and formation of secondary CuO phase. The effect of the dopant ion can be seen also by a close up view of the XRD patterns (fig. 3).

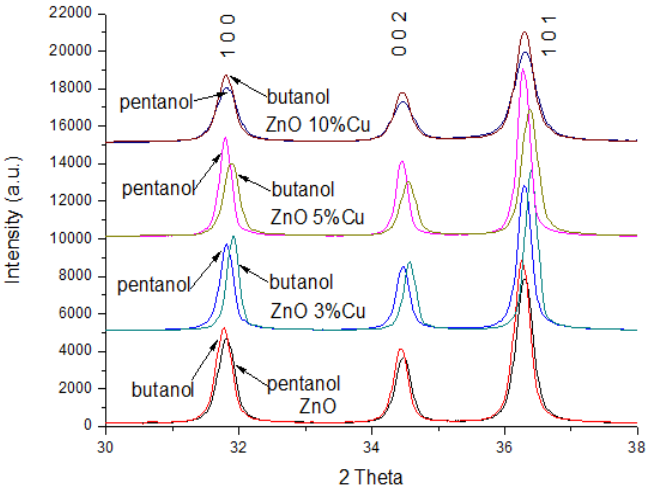

Fig. 3. Close up view of XRD patterns of undoped ZnO and Cu-doped ZnO powder samples at different doping levels 1, 3, 5 and 10%

It can be seen that while undoped and 10%Cu ZnO samples are similar regardless of the solvent used, for the 3% and 5% samples obtained in 1-butanol there is a noticeable shift of the peaks towards higher angle values.

The TEM bright field image, figure 4, for the 3% doped ZnO nanoparticles reveals that the powder is composed from polyhedral shaped particles, with an average particle size of approximately 100 nm. The nanopowder presents a tendency to form agglomerates. In the case of the sample synthetized in 1-pentanol an additional number of smaller

Alcohol \ Dopant	0% Cu	3% Cu	5% Cu	10% Cu
1-butanol	32.50	44.87	32.50	28.11
1-pentanol	29.96	38.90	44.95	22.06

Table 1
CRYSTALLITE SIZE (nm) FOR THE SYNTHETIZED NANOPOWDERS

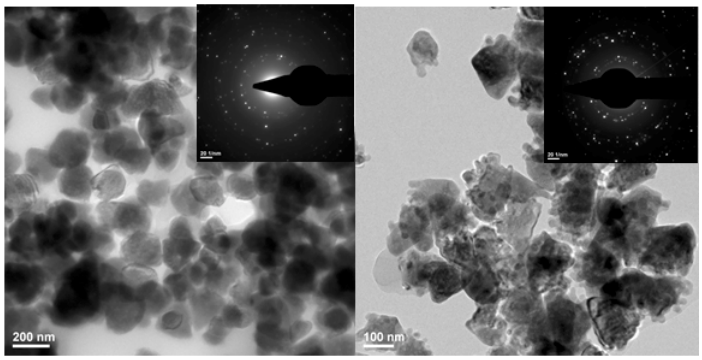

Fig. 4. TEM images of 3%Cu doped ZnO polyhedral shaped particles obtained in (A) 1-butanol and (B) 1-pentanol with the corresponding SAED pattern.

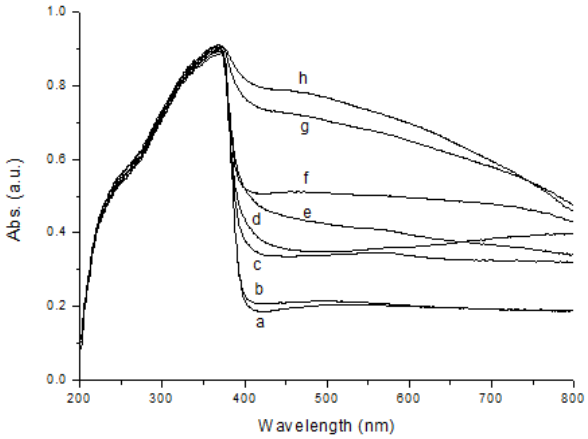

Fig. 5. Diffuse reflectance spectra for pure and doped ZnO in 1-butanol: 0%Cu_b; 3%Cu_c; 5%Cu_f; 10%Cu_g and in 1-pentanol: 0%Cu_a; 3%Cu_d; 5%Cu_e; 10%Cu_h.

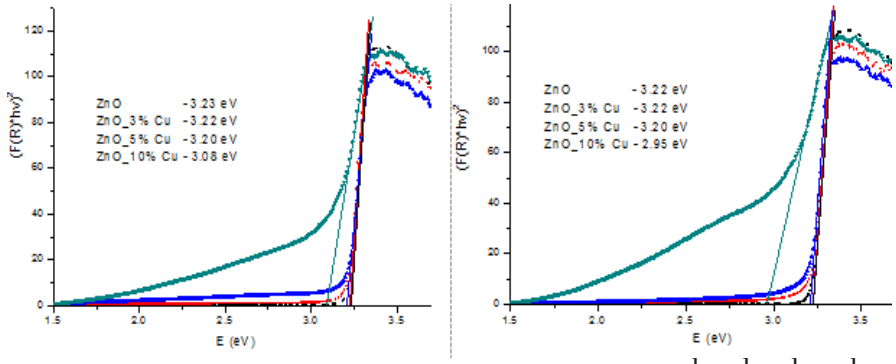

Fig. 6. Plot of the transformed Kubelka-Munk function vs. the energy (A) for the 1-butanol and (B) for the 1-pentanol syntheses

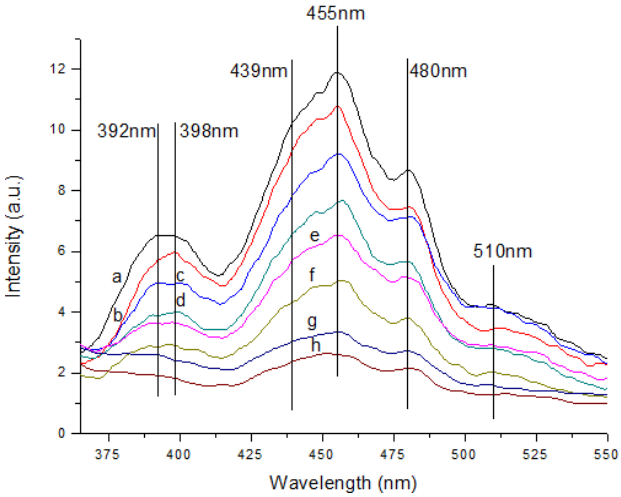

Fig. 7. Photoluminescence spectra for pure and doped ZnO in 1-butanol: 0%Cu_a; 3%Cu_c; 5%Cu_e; 10%Cu_g and in 1-pentanol: 0%Cu_b; 3%Cu_d; 5%Cu_f; 10%Cu_h

particles (of ~ 20nm size) can be seen on the edge of the larger particles. The HRTEM images, not presented here, shows clear lattice fringes of interplanar distances of d = 2.72 Å for nanocrystalline ZnO, corresponding to Miller indices of (1 0 0) crystallographic planes of hexagonal ZnO. In addition, the regular succession of the atomic planes indicates that the nanocrystalites are structurally uniform and crystalline with no amorphous phase present.

The electronic spectra recorded for pure and Cu-doped ZnO powder samples are presented in figure 5. As was expected along with the high absorbtion band in the UV domain that is characteristic for ZnO, an absorbtion broad band in visible domain is present due to the copper ions. With the increase of the dopant percentage the intensity of the visible absorbtion band is increasing.

The fundamental absorption refers to the optical transition of electrons from the valence band to conduction band and can be used to determine the nature and values of optical band gap of the nanoparticles. For analysis purposes the diffuse reflectance, *R*, of the sample can be related to the Kubelka-Munk function *F(R)* by the relation $F(R)=(1-R)^2/2R$ [16]. To determine the band-gap energies (Eg) for the ZnO powder samples, a plot of the square of the modified Kubelka-Munk function vs. the energy is presented in the figure 6. This yields the direct band gap energy [32]. The band-gap energies (Eg) for the Cu-doped ZnO powder samples are determined to be between 2.95-3.23 eV, by the extrapolation to $[F(R)\cdot h\nu]^2 = 0$. The calculated band gap for the Cu-doped ZnO powder samples is smaller than that for pure ZnO, which is in good agreement with the fact that doping ions will introduce new electronic levels inside the ZnO band gap.

The sharpest decrease of the band-gap energy is for the sample doped with 10%Cu in 1-pentanol, from 3.22 to 2.95eV.

The literature is abundant in reports of ZnO photoluminescence. The photoluminescence spectra of ZnO powders usually present two emission peaks in the UV and visible ranges. The UV emission corresponds to the near band-edge emission (NBE) and the visible emission is commonly referred to as a deep-level or trap-state emission [16].

The photoluminescence spectra results, figure 7, show that the as-synthesized samples have a wurtzite structure, with a weaker UV emission, two blue-green emissions, one centered at 455 nm (with a shoulder at 439 nm) and a second at 480 nm and a green emission around 510nm. The weak UV emission at 392-398nm is assigned to the free exciton emission from the wide band gap of ZnO (NBE). All the emission bands are becoming weaker as the dopant percentage is increasing, indicating the presence of non-radiative pathways of deactivating.

The results of the photocatalytic activity of the ZnO samples after 1 hour of irradiation are presented in figure 8. The samples synthetized in 1-butanol have in general a

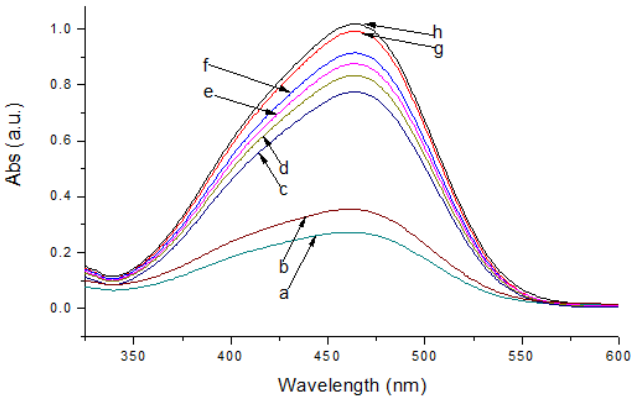

Fig. 8. Determination of photocatalytic activity after one hour of irradiation versus methyl orange for pure and doped ZnO in 1-butanol: 0%Cu_a; 3%Cu_c; 5%Cu_e; 10%Cu_g and in 1-pentanol: 0%Cu_b; 3%Cu_d; 5%Cu_f; 10%Cu_h

better photocatalytic activity than the samples obtained in 1-pentanol. The decreases of the intensity for the absorption maximums of methyl orange as the dopant percentage increase indicate that the photocatalytic activity is quenched by the presence of the copper ions. The pure ZnO samples are exhibiting the best photocatalytic activity, while the 10%Cu ZnO samples present almost no activity.

The decrease of the photocatalytic activity is most probably due to the blocking of the surface-active centers by the Cu^{2+} ions. There is a strong correlation between quenching of the photoluminescence emission and the decreasing of the photocatalytic activity.

Conclusions

In conclusion, we have prepared and characterized pure and Cu^{2+} doped ZnO nanopowders by solvothermal method in 1-butanol and 1-pentanol. The nanoparticles have a polyhedral morphology, with the diameter in the range of 100nm but with crystallite size of ~20-40nm. The optical properties indicate a good absorbance in UV-Vis domains that increases with the dopant percentage. The luminescence emission and the photocatalytic activity are decreasing as the percentage of Cu^{2+} ions is increasing. We report here for the first time to our knowledge the obtaining of Cu doped ZnO nanoparticles with negligible photocatalytic activity, which makes them suitable as UV shield in various applications as textile coating or cosmetic industry.

Acknowledgement: This paper is supported by the UEFISCDI through PN-II-PT-PCCA-2013-4-0891 project: Innovative dental products with multiple applications no. 229/2014

References

1.UNSOY, G., GUNDUZ, U., OPREA, O., FICAI, D., SONMEZ, M., RADULESCU, M., ALEXIE, M., FICAI, A., Current Topics in Medicinal Chemistry, **15**(16), 2015, p. 1622.
2.GINGASU, D., OPREA, O., MINDRU, I., CULITA, D.C., PATRON, L., Digest Journal of Nanomaterials and Biostructures, **6**(3), 2011, p. 1215.
3.FICAI, D., FICAI, A., VASILE, B.S., FICAI, M., OPREA, O., GURAN, C., ANDRONESCU, E., Digest Journal of Nanomaterials and Biostructures, **6**(3), 2011, p. 943.
4.VAJA, F., FICAI, D., FICAI, A., OPREA, O., GURAN, C., Journal of Optoelectronics and Advanced Materials, **15**(1-2), 2013, p. 107.
5.VAJA, F., OPREA, O., FICAI, D., FICAI, A., GURAN, C., Digest Journal of Nanomaterials and Biostructures, **9**(1), 2014, p. 187.
6.STROIA, A., COVALIU, C.I., OPREA, O., PASCU, L.F., JITARU, I., Rev. Chim. (Bucharest), **66,** no. 4, 2015, p. 511.
7.OPREA, O., VASILE, O.R., VOICU, G., ANDRONESCU, E., Digest Journal of Nanomaterials and Biostructures, **8**(2), 2013, p. 747.
8. OPREA, O., ANDRONESCU, E., FICAI, D., FICAI, A., OKTAR, F.N., YETMEZ, M., Current Organic Chemistry, **18**(2), 2014, p. 192.
9.GINGASU, D., MINDRU, I., PATRON, L., CULITA, D.C., CALDERON-MORENO, J.M., DIAMANDESCU, L., FEDER, M., OPREA, O., Journal of Physics and Chemistry of Solids **74**(9), 2013, p. 1295.
10.CULITA, D.C., SIMONESCU, C.M., DRAGNE, M., STANICA, N., MUNTEANU, C., PREDA, S., OPREA, O., Ceramics International, **41**(10), 2015, p. 13553.
11.GINGASU, D., MINDRU, I., CULITA, D.C., PATRON, L., CALDERON-MORENO, J.M., OSICEANU, P., PREDA, S., OPREA, O., PARVULESCU, V., TEODORESCU, V., WALSH, J.P.S., Materials Research Bulletin, **62**, 2015, p. 52.
12.MINDRU, I., GINGASU, D., PATRON, L., MARINESCU, G., CALDERON-MORENO, J.M., DIAMANDESCU, L., PREDA, S., OPREA, O., Ceramics International, **41**(4), 2015, p. 5318.
13.COVALIU, C.I., CHIOARU, L.C., CRACIUN, L., OPREA, O., JITARU, I., Optoelectronics and Advanced Materials-Rapid Communications, **5**(10), 2011, p. 1097.
14.VOICU, G., OPREA, O., VASILE, B.S., ANDRONESCU, E., Digest Journal of Nanomaterials and Biostructures, **8**(2), 2013, p. 667.
15.OPREA, O., GHITULICA, C.D., VOICU, G., VASILE, B.S., OPREA, A., Revista Romana De Materiale-Romanian Journal of Materials, **43**(4), 2013, p. 408.
16.OPREA, O., VASILE, O.R., VOICU, G., CRACIUN, L., ANDRONESCU, E., Digest Journal of Nanomaterials and Biostructures, **7**(4), 2012, p. 1757.
17.PALADE, S., PANTAZI, A., VULPE, S., BERBECARU, C., TUCUREANU, V., OPREA, O., NEGREA, R.F., DRAGOMAN, D., Polymer Composites, doi: 10.1002/pc.23744, 2015.
18.RADULESCU, M., COX, M., OANCEA, A.M.S., Solvent Extraction and Ion Exchange, **30**(4), 2012, p. 372.
19.OANCEA, A.M.S., POPESCU, A.R., RADULESCU, M., WEBER, V., PINCOVSCHI, E., COX, M., Solvent Extraction and Ion Exchange, **26**(3), 2008, p. 217.
20.LACATUSU, L., NICULAE, G., BADEA, N., STAN, R., POPA, O., OPREA, O., MEGHEA, A., Chemical Engineering Journal, **246**, 2014, p. 311.
21.NICULAE, G., BADEA, N., MEGHEA, A., OPREA, O., LACATUSU, I., Photochemistry and Photobiology, **89**(5), 2013, p. 1085.
22.LACATUSU, I., BADEA, N., STAN, R., MEGHEA, A., Nanotechnology, 23, 2012, p. 4555702.
23.RADULESCU, M., FICAI, D., OPREA, O., FICAI, A., ANDRONESCU, E., HOLBAN, A.M., Current Pharmaceutical Biotechnology, 16(2), 2015, p. 128.
24.VASILE, B.S., OPREA, O., VOICU, G., FICAI, A., ANDRONESCU, E., TEODORESCU, A., HOLBAN, A., International Journal of Pharmaceutics, 463(2), 2014, p. 161.
25.RUSU, L.C., NEDELCU, I.A., ALBU, M.G., SONMEZ, M., VOICU, G., RADULESCU, M., FICAI, D., FICAI, A., NEGRUTIU, M.L., SINESCU, C., Journal of Nanomaterials, doi: 10.1155/2015/361969, 2015, p. 361969.
26.PELMUS, M., OPREA, O., STANESCU, M.D., U.P.B. Sci.Bull.,Series B, 77(3), 2015, p. 73.
27.MARINESCU, G., CULITA, D.C., PATRON, L., NITA, S., MARUTESCU, L., OPREA, O., Rev. Chim. (Bucharest), **65**, no. 12, 2014, p. 1421.
28.MARINESCU, G., CULITA, D.C., PATRON, L., NITA, S., MARUTESCU, L., STANICA, N., OPREA, O., Rev. Chim. (Bucharest), **65**, no. 4, 2014, p. 426.
29.VOICU, G., OPREA, O., VASILE, B.S., ANDRONESCU, E., Digest Journal of Nanomaterials and Biostructures, 8(3), 2013, p. 1191.
30.OANCEA, A.M.S., RADULESCU, M., OANCEA, D., PINCOVSCHI, E., Industrial & Engineering Chemistry Research, **45**(26), 2006, p. 9096.
31.OANCEA, A.M.S., RADULESCU, M., PINCOVSCHI, E., COX, M., OANCEA, D., Solvent Extraction and Ion Exchange, **23**(1), 2005, p. 131.
32.OPREA, O., ANDRONESCU, E., VASILE, B.S., VOICU, G., COVALIU, C., Digest Journal of Nanomaterials and Biostructures, 6(3), 2011, p. 1393.
33.VASILE, O.R., SERDARU, I., ANDRONESCU, E., TRUSCA, R., SURDU, A.V., OPREA, O., ILIE, A., VASILE, B.S., Comptes Rendus Chimie, http://dx.doi.org/10.1016/j.crci.2015.08.005, 2015

Manuscript received: 7.12.2015